Int. J. Environ. Sci. Technol.
DOI 10.1007/s13762-017-1494-9

ORIGINAL PAPER

Lanthanides removal from mine water using banana peels nanosorbent

O. A. Oyewo[1] · M. S. Onyango[1] · C. Wolkersdorfer[2,3]

Received: 22 December 2016 / Revised: 1 April 2017 / Accepted: 22 July 2017

Abstract This study focuses on the performance of nanostructured banana peels in lanthanide-laden mine water treatment. Specifically, nanostructure formation via mechanical milling, characterization in detail and application of this sorbent media in rare earth elements (REEs) removal from synthetic and real mine water are thoroughly investigated. The sorbent samples were characterized by transmission electron microscopy, Brunauer–Emmett–Teller, X-ray diffraction and Fourier transform infrared analyses, while the amount of REEs adsorbed was analysed using inductively coupled plasma optical emission spectroscopy. Results revealed that the particle and crystallite sizes were reduced from <65,000 to <25 nm and 108 to 12 nm, respectively, as the milling progressed. Furthermore, the fracture of particles resulted in a surface area increment from 1.07 to 4.55 $m^2\ g^{-1}$. Through Fourier transform infrared analysis, the functional groups responsible for the coordination and removal of metal ions were found to be carboxylic group (at absorption bands of 1730 cm^{-1}) and amine groups (889 cm^{-1}). The Langmuir maximum adsorption capacity was 47.8 mg g^{-1} for lanthanum and 52.6 mg g^{-1} for gadolinium. Meanwhile, results revealed that banana peels have a high affinity for Sm, Eu, Nd, Pr, Gd, Tb and Lu compared to other lanthanides present in the mine water samples. The results obtained so far indicate that nanostructured banana peel is a potential adsorbent for REEs removal from mine water. However, for any application, the water matrix to be treated substantially influences the choice of the sorbent material.

Keywords Agricultural waste · Batch adsorption · Mechanical milling · Rare earth elements · Mine water

Editorial responsibility: B.V. Thomas.

✉ O. A. Oyewo
atiba.opeyemi@gmail.com

[1] Department of Chemical, Metallurgical and Materials Engineering, Tshwane University of Technology, Pretoria 0001, South Africa

[2] SARChI Chair for Mine Water Management, Department of Environmental, Water and Earth Sciences, Tshwane University of Technology, Pretoria 0001, South Africa

[3] Laboratory of Green Chemistry, Lappeenranta University of Technology, Sammonkatu 12, 50130 Mikkeli, Finland

Introduction

Rare earth elements (REEs) have unique properties that inherently make them useful in nuclear reactors, superconductors and super-magnets. Moreover, REEs are also useful in the energy and environmental sectors (Marwani et al. 2013). Lanthanum and gadolinium as examples of REEs have attracted cumulative attention based on their unique physical and chemical properties, as well as their constant demands for advanced new materials production, especially nuclear reactors (Rao and Biju 2000; Kondo and Kamio 2002). These two elements are majorly extracted from monazite ores by treating the ores with hot concentrated H_2SO_4 and specifically used as catalysts in glass production, petroleum, medicinal purposes, mineral identification and neutron radiography (Kondo and Kamio 2002). They can also be used in magnets, phosphors, lamps, superconductors and optoelectronic applications. As the extraction of these REEs continues due to their higher industrial demand, they find their way into mine water or ore processing effluents and might pose a serious risk to human and aquatic life (Pagano et al. 2016) based on their bioavailability. Most previous pollution control-related

Published online: 03 August 2017

research and development mainly focused on assessing metal recovery possibilities; however, polishing effluents before discharge to protect the environment and human health is also critically important.

Several researchers have used various techniques such as solvent extraction, organic and inorganic ion exchanger, micellar ultrafiltration, chemical precipitation and adsorption in mine effluent treatment. Chemical precipitation techniques are reliable treatment methods but need large storage facilities for the precipitated sludge and sometimes require additional treatment options (Wolkersdorfer 2008). Ion exchange, which is expensive and sophisticated, would allow metallic ions recovery (Dorota and Zbigniew 2012). Adsorption processes are highly economical and capable of removing contaminants even at trace level. The use of this technique in water and wastewater treatment due to its simplicity, low cost of operation and wide end use is reported (Naeem et al. 2007). However, the performance of any adsorption process is highly dependent on the choice of appropriate media. For lanthanides removal from aqueous solutions, various potential adsorbent materials are investigated by different research groups. These materials include alginate–chitosan gel beads, Lewatit TP 214 resin, pyridine resin, chemically modified polyurethane foam and agricultural wastes (Dongbei et al. 2010; Nacer et al. 2014; Tatsuya et al. 2013).

A fibrous agricultural waste such as sugarcane bagasse, pineapple peels, coconut coir, apple and banana peels (Bakiya and Sudha 2012) has been shown to be a potential adsorption media for metal ions removal from wastewater. This is possible due to the presence of beneficial constituents and acid groups such as cellulose, carboxylic and phenolic groups that are necessary for the effective treatment. The presence of an additional amine group in banana peel improves the latter's ability to adsorb metal ions as compared to other agricultural products. Furthermore, the reusability of banana peels up to 11 times without replacement has been reported; therefore, the regeneration of this material is highly possible (Castro et al. 2011). Though many investigations have been done on the usage of banana peels in waste water treatment (Achak et al. 2009; Bankar et al. 2010; Firas 2013), it is obvious that the efficiency of any sorbent media mostly depend on its particle size.

Advances in nanoscience and nanotechnology have expanded the ability to develop nanomaterials with enhanced properties to solve the current problems in water treatment. As a result of their small size, nanomaterials can exhibit an array of unique novel properties which can be utilized in the development of new metal treatment technologies and improvement of existing ones (Arup and Jayanta 2015). Castro et al. (2011) reported the use of banana peels in micro size of 35–45 μm with an adsorption capacity of 20 mg g^{-1} for copper removal from aqueous solution. Other researchers combined banana peels with a polymer to develop new sorption media, which unfortunately had very low adsorption performance (Ashok et al. 2010). A number of adsorption studies have shown that improved surface area and access as well as the number of active sites relate to the performance of the adsorption media. In this regard too, we speculated that there is a possibility of improved performance of banana peels in metal ions removal from water if this agricultural resource is reduced to nanosize in order to increase its surface area which can as well increase the accessibility of adsorptive sites.

Therefore, in this study, the main objective was to reveal more information on the characterization of banana peel nanosorbent as well as its efficiency in REEs removal from mine water. Lanthanum and gadolinium removal performances from aqueous solution were investigated in batch adsorption mode, and moreover, the banana peels nanosorbent (BPN) performances in all REEs present in real mine water were explored.

Materials and methods

Banana peel (*Musa* × *paradisiacal*) samples were obtained, cut into smaller pieces and double-washed with distilled water to remove the adhering dirt and then sun-dried for 10 days. The dried peels were crushed and screened up to a particle size of up to 65 μm. Acid and alkali treatments were then done. First, banana peels were soaked in 2 M NaOH for 6 h and later rinsed to remove excess chemicals. The same procedure was then applied in acid treatment using 5% nitric acid. Before air drying, the treated banana peels were rinsed until the pH was neutral. This was done to enhance the peels' sorption capacity. The chemicals used such as NaOH and HNO_3 were obtained from Sigma-Aldrich, South Africa. All chemicals used were of analytical grade.

Mechanical milling of crushed banana peels (up to 65 μm) was conducted in a planetary continuous ball mill machine (PM 100 CM) at a constant speed of 200 rpm (rotations per minute) using ethanol as process control agent at room temperature. Agate vial and balls were used to avoid contamination by debris if any. To prevent heat effects during milling, the planetary continuous milling machine was automatically fixed to cool down for 15 min after 2-h milling intervals. The milling was done for 30 h, and the samples were taken at 10-h intervals. Batch equilibrium experiments were performed to determine the adsorptive performance of banana peels nanosorbent (BPN) in lanthanides removal from synthetic and mine water. In the first adsorption experiment, the effect of solution pH was studied to determine the optimum pH for the process. Using either NaOH (0.1 M) or HCl (0.1 M),

the initial pH adjusted from 2 to 10 and 0.1 g of BPN was added to 100-mL plastic bottles containing 50 mL solution of 100 mg L^{-1} lanthanides synthetic water. Thereafter, the bottles were placed in a thermostatic shaker operated at 200 rpm for 24 h. At the end of the contact period, the samples were filtered using a syringe filter of 0.45 µm pore size and the filtrate analysed by inductive coupled plasma optical emission spectroscopy (ICP-OES) to determine the concentration of lanthanides in aqueous solution (lanthanum and gadolinium) while mine water filtrate was analysed by inductive coupled plasma mass spectrometer (ICP-MS). The above procedure was repeated to determine the effect of initial concentration, sorbent mass and temperature on the amount of lanthanides adsorbed on BPN. The effect of sorbent loading was explored by varying the mass of the sorbent from 0.01 to 0.3 g, while the effect of concentration was explored by varying the initial concentration of the lanthanides synthetic solution from 20 to 200 mg L^{-1}. Finally, between 25 and 45 °C the temperature was varied to investigate its effect. The sorbent mass was fixed at 0.2 g for the latter experiments.

The percentage removal efficiency R_t was calculated (Eq. 1) as well as the equilibrium uptake q_e (mg g^{-1}), Eq. 2:

$$R_t = \frac{C_o - C_e}{C_o} \times 100 \tag{1}$$

$$q_e = \frac{C_o - C_e}{m} \times V \tag{2}$$

where C_o (mg L^{-1}) is the initial lanthanides concentration, C_e (mg L^{-1}) the lanthanides equilibrium concentration, V is the volume of the sample (L) and m is the adsorbent mass (g).

Langmuir and Freundlich models were used for equilibrium isotherm data interpretation. The linearized Langmuir (Eq. 3) and Freundlich (Eq. 4) adsorption isotherm equations are given by:

$$\frac{C_e}{q_e} = \frac{1}{q_o b} + \frac{C_e}{q_o} \tag{3}$$

$$\log q_e = \log K_F + \frac{1}{n} \log C_e \tag{4}$$

where b is the Langmuir constant, q_o is the Langmuir maximum adsorption capacity, n and K_F are the Freundlich parameters that relate to adsorption intensity and adsorption capacity, respectively.

Method of adsorbents characterization

The crystallinity of the adsorbent material was determined by X-ray diffraction (XRD) analysis via the high score plus programme. The PROFILE-FIT package (Mhadhbi et al. 2010) was used to determine BPN crystalline sizes at different milling times. Moreover, the physical profiles such as width broadening of the peaks were determined from the measured intensity profile. The crystalline size of as-received and the milled samples were then calculated from the integral width of the physical broadening profile by the Scherrer equation (Eq. 5):

$$\tau = \frac{K\lambda}{\beta \cos\theta} \tag{5}$$

where τ is the mean size of the ordered (crystalline) domains, which may be smaller or equal to the grain size; β is the line broadening at half the maximum intensity (FWHM) after subtracting the instrumental line broadening in radians, θ is the Bragg angle and K is a dimensionless shape factor with a value close to unity; λ is the X-ray wavelength.

The particle sizes were determined by transmission electron microscopy (TEM) analysis using a JEM-2100F field emission electron microscope run at 200 kV and the particle size distribution analysis using WSxM 5.0 software (Horcas et al. 2007). Changes in surface area during milling were obtained by Brunauer–Emmett–Teller (BET) analysis using a micrometrics TriStar II 3000 (USA) surface area analyser. The Fourier transform infrared spectroscopy (FTIR) analysis was done to identify the key functional groups responsible for the material to coordinate and remove REEs using a PerkinElmer Spectrum 100 spectrometer with the spectra recorded in the 500–4000 cm^{-1} range at a resolution of 4 cm^{-1}.

Results and discussion

Characterization of adsorbents

Fourier transform infrared (FT-IR) spectroscopy

The FT-IR spectra of crushed banana peels, 10-, 20- and 30-h-milled BPN as well as used 30-h-milled BPN show bands at 3486–3286 cm^{-1} which are attributed to O–H stretching while the C–H stretching are identified at 2920–2951 cm^{-1} (Fig. 1). The band at 1730 cm^{-1} is attributed to the C=O bond of carboxylic acid (Annadurai et al. 2003), and the wavelength of this band becomes lower as the milling progressed suggesting that this phase might be sensitive to mechanical stress (Oyewo et al. 2016). The change in wavelength of the band at 1435 cm^{-1} was noticed in the after-use form suggesting the interaction between lanthanides and hydrophilic surface of BPN. The band at 889 cm^{-1} is attributed to the amine group, and as can be seen, this band disappears in the after-use BPN media, indicating that the amine group is majorly responsible for the removal of lanthanides ions.

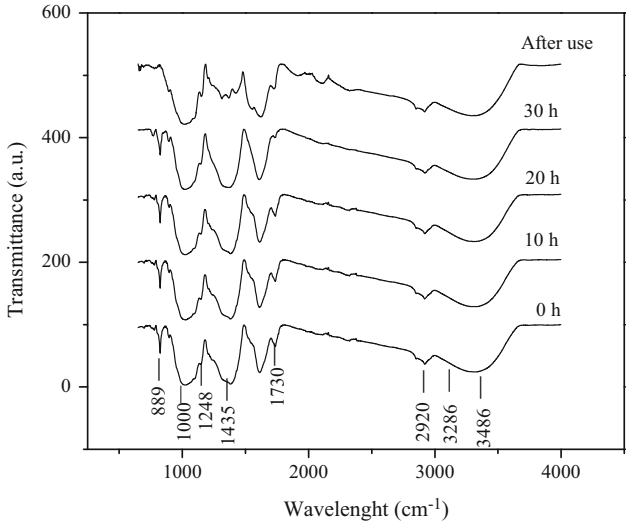

Fig. 1 FT-IR Spectra of banana peels at different milling times and after lanthanides adsorption (after-use form) (from Oyewo et al. 2016)

$$Ln^{+3}_{(aq)} + 3\ NH_2^- \rightarrow\ Ln(NH_2)_3 \qquad (6)$$

Brunauer–Emmett–Teller (BET) surface area analysis

The adsorbents' surface area was analysed using the BET method and was found to be 1.07 $m^2\ g^{-1}$ for crushed banana (smaller than 65 µm). The surface area increased as the milling time increased to 30 h (4.55 $m^2\ g^{-1}$) which may be due to further fracturing of the particles (Table 1). Generally, one of the common characteristics of carbonaceous materials is their low surface area compared to silica-based materials and BPN is not exceptional (Hossain et al. 2012). Increased surface area has inherent advantage of exposing more active sites on an adsorption material, which feature may result in enhanced adsorption of water contaminants.

Transmission electron microscopy (TEM)

Changes in average particle size at different milling times were analysed by TEM (Fig. 2a–d). As can be seen, the average particle size changes prominently during the mechanical milling. Increase in milling time (0–10 h) results in a decrease in particle size from below 65 µm to around 100 nm, and from 100 to 50 nm after 20 h and finally from 50 to 15 nm after 30-h milling time. This confirms the nanostructure (0–100 nm) formation.

Particle size distribution

Particle size distribution analyses are very important in the mechanical milling of any material for accurate particle size analysis. This analysis provides a quantitative description of the range of particle size present in the powders. In this specific case, the analysis was done for the description of particle size ranges in banana peel samples at different milling times. The particle size distribution technique was used in analysing images obtained from transmission electron microscopy (TEM). This technique was used to overcome the limitations of traditional methods used for determining mean particle size distribution of powder materials (Suryanarayana 2001). It was done by selecting the entire particle region in the image, and the particle data were extracted from the image for particles dimension determination of the 10-h-milled BPN (<300 nm), 20-h-milled BPN (<65 nm) and 30-h-milled BPN (<25 nm) (Fig. 3). It was observed that as the milling progressed, the fracturing of the particles increased and more nanoparticles were formed. Clearly, mechanical milling results in smaller particle sizes of BPN which is a necessary precondition for a good adsorption media.

X-ray diffraction (XRD) analysis

The results of the X-ray diffraction (XRD) analysis of the banana peels before and after different milling times are shown in Fig. 4. Prior to milling, banana peels displayed an amorphous character with a certain degree of crystallinity which can be seen as a bump at a 2θ angle between 10° and 50°; within the same range, very clear peaks are observed at 2θ angles of 20° and 23°; the latter is also present after milling but with reduced intensity (Suryanarayana 2001). This suggests reduction in the amount of corresponding phase ($C_{84}H_{12}N_{16}O_{16}$). The bump (amorphous) disappeared as the milling proceeded, indicating that the material becomes purely crystalline due to its nanostructure (Heguang et al. 2015). Noticeable transformation features occurred in the banana peels powder during milling such as crystallite size reduction which brought about an increase

Table 1 BET analysis of banana peels nanosorbent

Sample name	Milling time (h)	Single point surface area ($m^2\ g^{-1}$)	BET surface area ($m^2\ g^{-1}$)
Crushed BPF	0	0.096	1.069
Milled BPN	10	2.004	2.204
Milled BPN	20	3.055	3.255
Milled BPN	30	4.156	4.555

BPF banana peels fine particles, *BPN* banana peels nanosorbent

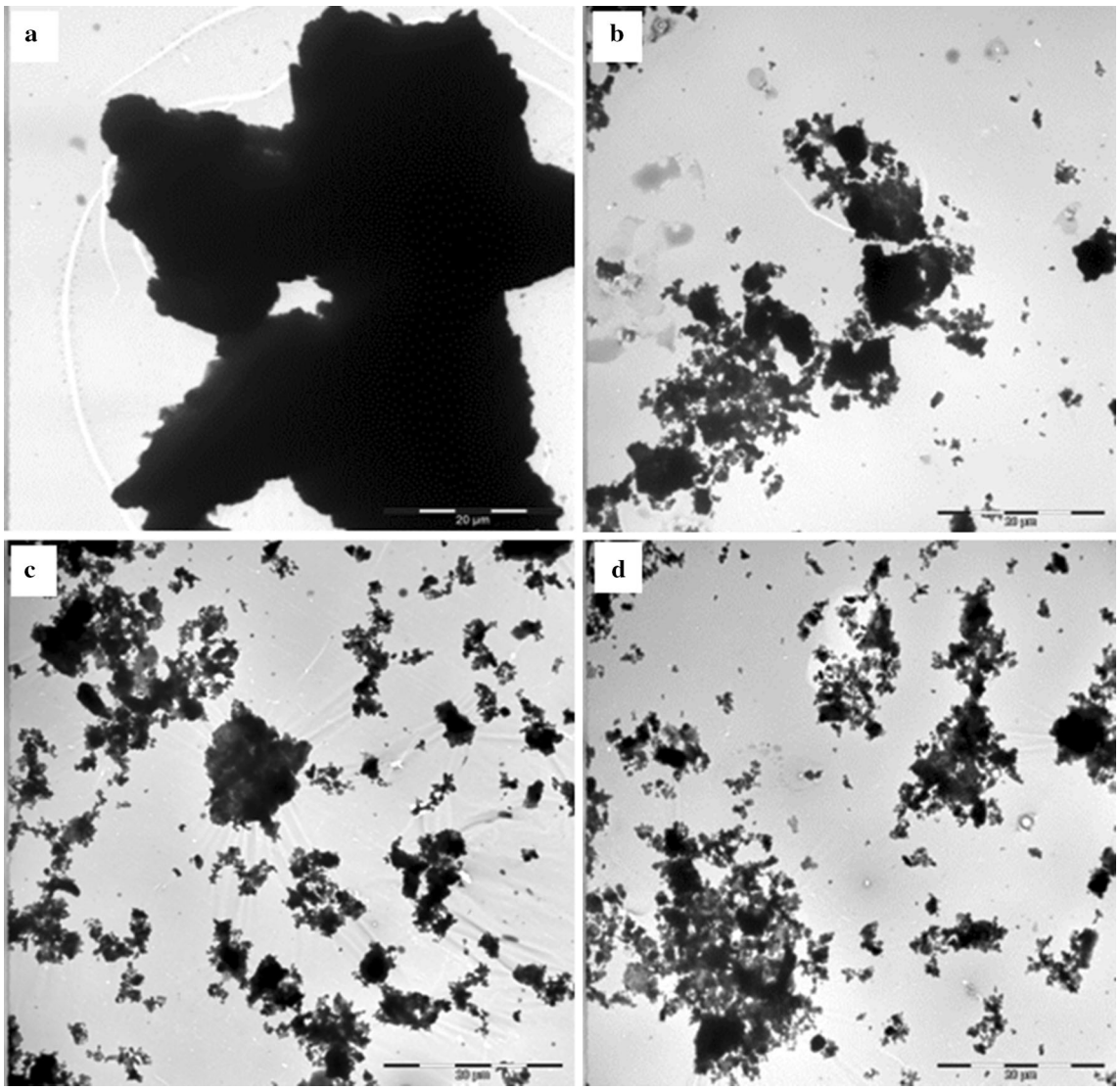

Fig. 2 TEM images of banana peels particles: **a** crushed, **b** 10-h milled sample, **c** 20-h milled sample, **d** 30-h milled sample

and a decrease in intensity of some peaks as revealed through the XRD scan at different milling time (Ungar 2004). Additionally, the increase in broadening and intensity of the peaks with milling time can be clearly seen, and this is an indication of a decrease in crystallite size as the milling progresses (Bushroa et al. 2012). The peak at 35° (2θ) shifted and was smaller in crushed powder indicating larger crystallite size in this sample. A number of phases are identified in BPN, and the prominent peaks correspond to amine and carboxylic groups which are the main groups responsible for its ability to remove metal ions (Hossain et al. 2012). The peaks attributed to $C_6Ca_6O_{18}$, $C_4H_{16}N_4$ and calcium become broader and visible as the milling time increased, whereas in the case of the crushed powder, no such phases are present. This might be due to further deformation of banana peel particles as a result of continuous milling. The appearance of new peaks in the milled samples such as $C_4H_4O_8$ indicates the formation of new phases as a result of continuous milling and ethanol used as a process control for wet milling.

The crystallite size (Table 2) decreases from 108 to 12 nm as milling time increases. This is due to continuous broadening of the peaks as the milling progressed resulting in a decrease in crystallite size (Venkateswarlu et al. 2014).

Analysis of mine water

Acid mine drainage samples were obtained from the dams near gold mine locations in South Africa situated in the North West Province and chemically analysed (Table 3). It was observed that some of these metal ions were also removed by adsorption on BPN. The pH and electrical

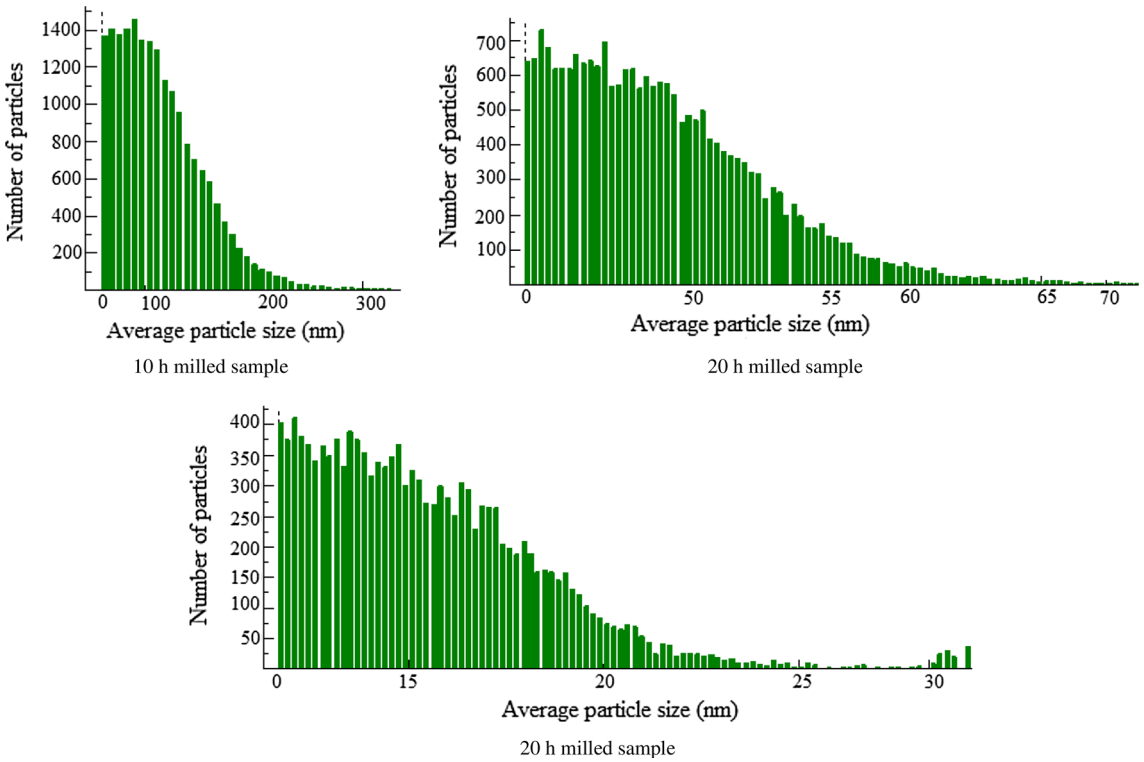

Fig. 3 Particle size distribution of banana peels nanosorbent: **a** 10-h milled sample, **b** 20-h milled sample, **c** 30-h milled sample

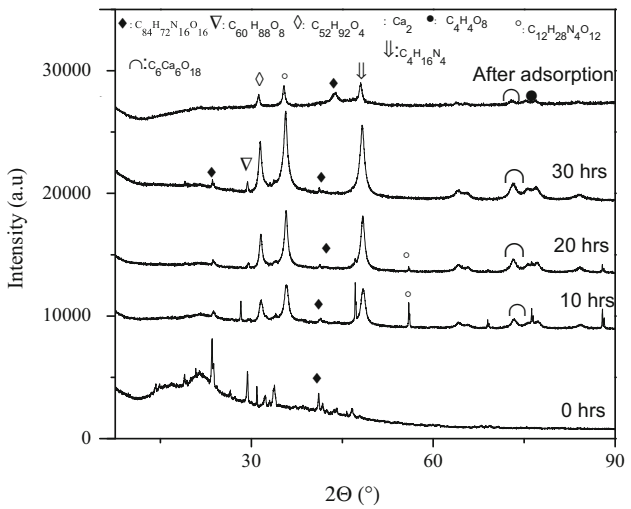

Fig. 4 XRD pattern of banana peels at different milling times and after lanthanides adsorption (after-use form) (from Oyewo et al. 2016)

Table 2 Summary of TEM and particle size distribution analyses of milled banana peels

Milling time (h)	Average particle size (nm)	Mean crystalline size (nm)	Lattice strain (%)
0	<65,000	108	0.24
10	<300	71	0.63
20	<65	20	0.64
30	<25	12	0.69

conductivity of these samples were measured and, respectively, recorded to be 3.18 and 2.2 mS cm^{-1} at location 1, and 3.86 and 14.16 mS cm^{-1} at location 2. The samples were stored in a cold room below 5 °C without further preservation to keep the chemical composition as close as possible to the original. It can be clearly seen that the different metal concentrations in both samples resulted from the different mine water matrix.

Adsorption results

Effect of initial solution pH

As can be clearly seen from the results, the lanthanides uptake increases between pH 2 and pH 4 and thereafter remains relatively constant (Fig. 5). This is because at acidic pH levels, hydrogen ions in the solution compete with the metal ions resulting in low adsorption of the metal ions, and by increasing the pH value, the adsorption increases due to reduced competition from hydrogen ions. The adsorption capacity remains relatively constant at pH > 5.2. Consequently, subsequent experiments were performed at pH 5.2. Meanwhile, in metal removal from aqueous solution, multiple mechanisms are involved in the sorption at high pH values. It is therefore not surprising that lanthanides adsorption onto BPN within the pH range of 8–10 was high. It is possible that both adsorption and

Table 3 Characterization of mine water concentration from two different locations; pH without units

Element, parameter	Location 1 (μg L^{-1})	Location 2 (μg L^{-1})
pH	3.18	3.86
La	248.33	3.11
Ce	791.40	12.44
Pr	63.38	3.42
Nd	235.68	27.24
Sm	46.83	12.62
Eu	10.65	4.04
Gd	55.35	23.43
Tb	8.27	4.70
Dy	43.31	29.35
Ho	8.40	6.62
Er	22.15	18.67
Tm	2.85	2.47
Yb	16.55	13.03
Lu	2.43	2.08
Li	143	4094
Mg	50,052	188,643
Al	29,369	7589
K	8655	37,460
Ca	15,193	398,398
V	8	91
Cr	99	35
Fe	23,435	63,436
Mn	27,703	16,071

precipitation mechanisms were involved (Nwe Nwe et al. 2008).

Effect of sorbent mass

Increasing the adsorbent dosage resulted in an increased lanthanides percentage removal (Fig. 6). This is because active sites available for lanthanides sorption are proportional to the adsorbent mass. Overall removal achieved in lanthanides sorption onto BPN in this study is higher compared with those reported elsewhere (El-Sofany 2008).

Adsorptive performance of BPN in lanthanides removal from real mine water

The experiments with real mine water were performed without pH adjustment to avoid the precipitation of iron ox-hydride present in the mine water samples; therefore, pH was measured and recorded (Table 3). It must be recognised that at the pH values of the mine waters (Table 3), adsorption processes may be limited due to hydrogen ions and other constituents competing for the available active sites on the surface of BPN. The

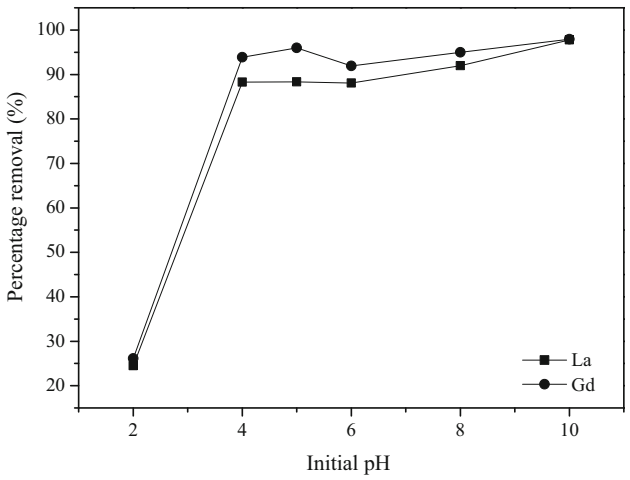

Fig. 5 Effect of solution pH in lanthanides synthetic water onto banana peels nanosorbent (BPN) (temp. 25 °C, duration 24 h, initial conc., 100 mg L^{-1} and sorbent mass 0.1 g)

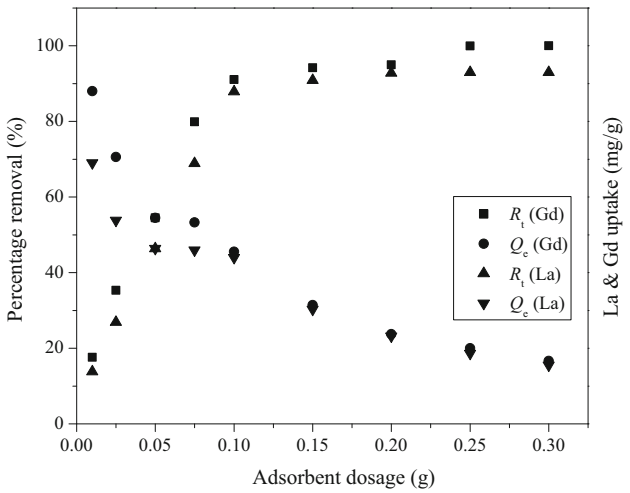

Fig. 6 Effect of adsorbent dosage on lanthanides adsorption (synthetic water; initial conc. 100 mg L^{-1} and pH 5.20, Temp. 25 °C, duration 24 h)

experiments' results showed that in location 1 the percentage removal of La onto BPN was very low (4%) compared to other lanthanides present in the sample (Figs. 7, 8). This was also noticed in location 2, where about 25% removal of La was observed, and this indicates that BPN has a low affinity for La compared to other lanthanides in these mine water samples. Generally, it can be clearly seen that BPN has a high affinity for Sm, Eu, Nd, Pr, Gd, Tb and Lu compared to the other lanthanides present in the samples.

A similar sorptive performance was also observed in Gd and Tb removal in the mine waters from these two locations, and this might be due to their similarities in physical and chemical properties based on lanthanides basicity series: $La^{3+} > Ce^{3+} > Pr^{3+} > Nd^{3+} > Pm^{3+} > Sm^{3+} >$

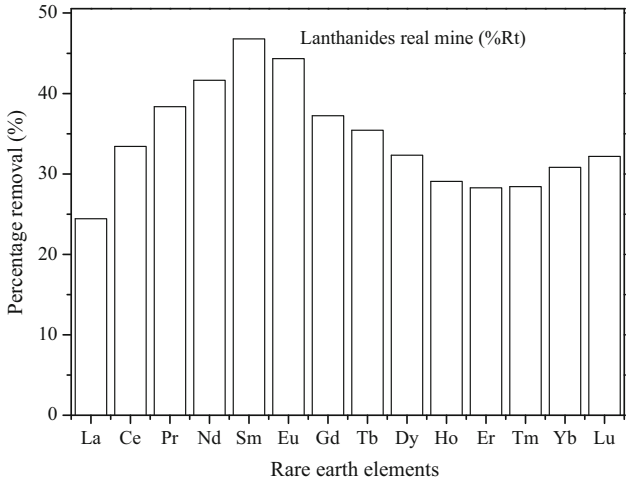

Fig. 7 Adsorptive performance of BPN in mine water from location 1 (pH 3.18, Temp. 25 °C, duration 24 h, dosage 0.25 g)

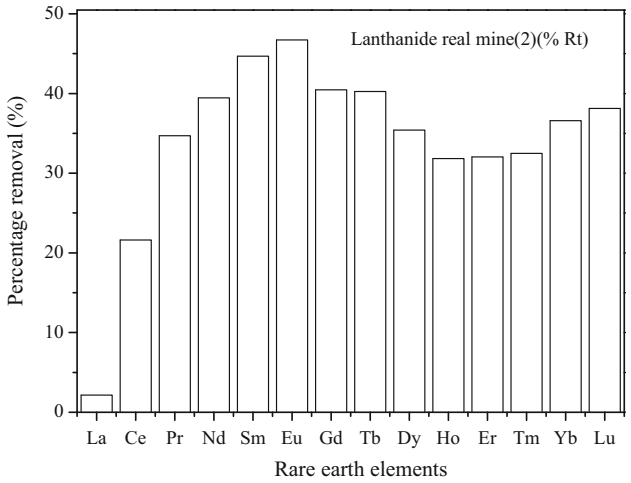

Fig. 8 Adsorptive performance of BPN in mine water from location 2 (pH 3.86, temp. 25 °C, duration 24 h, dosage 0.25 g)

$Eu^{3+} > Gd^{3+} > Tb^{3+} > Dy^{3+} > Ho^{3+} > Er^{3+} > Tm^{3+} > Yb^{3+} > Lu^{3+}$ (Rao and Biju 2000).

Sorption isotherms

The temperature range of 25–45 °C was explored in lanthanum and gadolinium sorption to determine the temperature dependence of the process in synthetic waters (Figs. 9, 10). It was clearly observed that an increase in equilibrium concentration results in an increase in lanthanides equilibrium uptake. Moreover, an increase in temperature also increased the adsorption capacity, indicating that lanthanides sorption onto BPN is a temperature-dependent process. The enhanced sorption at higher temperatures may occur due to a decrease in the thickness of the boundary layer surrounding the BPN. There is also a possibility of an increase in the

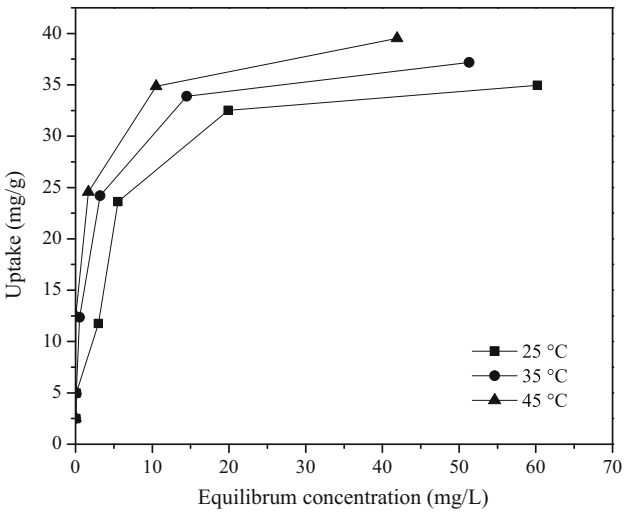

Fig. 9 Isotherms for lanthanum sorption onto BPN (pH 5.2, duration 24 h, initial conc. 20 mg L^{-1}, 200 mg L^{-1} and sorbent mass 0.2 g)

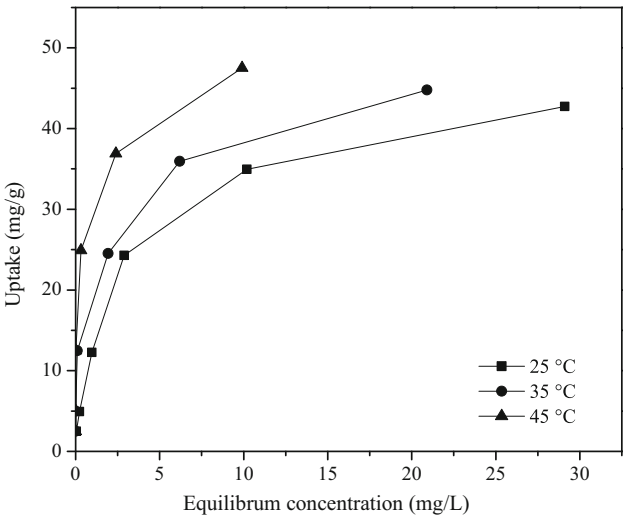

Fig. 10 Isotherms for gadolinium sorption onto BPN (pH 5.2, duration 24 h, initial conc. 20 mg L^{-1}, 200 mg L^{-1} and sorbent mass 0.2 g)

movement of the molecules with a rise in temperature. The data provided from the sorption equilibrium are used to describe the interaction between lanthanides and BPN for effective design of an adsorption process. Furthermore, sorption equilibrium data are used in comparing the performance of different media for a given sorption process. Subsequently, the existing mathematical models, such as Langmuir and Freundlich, were used for the experimental analyses (Table 4). In comparing these two well-known models in terms of correlation coefficients (R^2), both isotherms described the gadolinium removal excellently, while lanthanum removal was described by the Langmuir isotherm only. Therefore, based on the isotherm modelling results, it may be argued that lanthanum adsorption occurred at

Table 4 Isotherms parameters for synthetic lanthanum and gadolinium adsorption onto banana peels nanosorbent

	Lanthanum			Gadolinium		
Langmuir isotherm parameters						
Temperature (°C)	q_m (mg g^{-1})	b (L mg^{-1})	R^2	q_m (mg g^{-1})	b (L mg^{-1})	R^2
25	38.8	2.6	0.992	46.2	2.1	0.995
35	42.5	1.3	0.999	48.6	0.7	0.991
45	47.8	0.8	0.999	52.6	0.2	0.995
Freundlich isotherm parameters						
	K_F (L g^{-1})	1/n	R^2	K_F (L g^{-1})	1/n	R^2
25	10.1	0.33	0.777	19.0	0.26	0.998
35	20.8	0.16	0.932	21.4	0.25	0.999
45	23.3	0.14	0.996	31.6	0.18	1.000

Table 5 Comparison of banana peels adsorption capacity with other adsorbents for removal of lanthanides from aqueous solution

Adsorbent	q_m (mg g^{-1})	References
Aliquat 336 impregnated onto Amberlite XAD-4 (La)	4.76	El-Sofany (2008)
Aliquat 336 impregnated onto Amberlite XAD-4 (Gd)	4.44	El-Sofany (2008)
Polyacrylamide stannic molybdophosphate	24.66	Abdel-Galil et al. (2016)
Platanus orientalis	28.7	Sert et al. (2008)
Banana peels bigger particles (La)	30.1	This study
Banana peels bigger particles (Gd)	35.6	This study
Banana peels nanosorbent (La)	47.8	This study
Banana peels nanosorbent (Gd)	52.6	This study

specific homogenous sites while gadolinium adsorption results suggest both homogenous and heterogeneous adsorption on the surface of BPN. The results further show that q_o, which measures the monolayer capacity of the adsorbent and the predicted K_F values from the Freundlich isotherm, increases as the temperature increases, while the Langmuir constant b decreases with an increase in temperature. This confirms enhanced sorption of these metals at higher temperature. The comparisons of BNP with other materials (Table 5) show that the newly developed material in this study is competitive.

Conclusion

In this study, nanostructure formation of banana peel as an adsorbent for REEs has been demonstrated. The particle size ranges were found to be controlled primarily by the milling time. The crystallinity and phase changes in banana peel via mechanical milling were investigated, and the crystallite size was found to decrease from >100 to 12 nm. Similarly, the particle size decreased from below 65 µm to below 25 nm as a function of milling time. The surface area increment of crushed banana peels powder (1.07–4.55 m^2 g^{-1}) was observed as milling time increased (0–30 h). Amine and carboxylic groups were found to be responsible for the ability of BPN to remove lanthanides from mine water. Moreover, the extent of adsorption was controlled primarily by pH and temperature. A solution pH of 5.20 was adopted for the sorption of lanthanides from synthetic water, which is consistent with the chemical interaction between the hydrophilic surface of BPN and the strongly electropositive lanthanides species. It was observed that a dosage of 0.3 g of BPN was required for 94 and 100% removal of lanthanum and gadolinium, respectively, from 100 mg L^{-1} initial concentration (aqueous solution) at pH 5.20. Meanwhile, the pH and electrical conductivity of two mine water samples were measured and found to be 3.18, 2.2 and 3.86, 14.2 mS cm^{-1} in location 1 and location 2, respectively. For these samples, it was observed that a dosage of 0.25 g of BPN was required for 40 and 45% removal of Nd, Gd, Tb, Sm and Eu in both locations, respectively. La removal was 25% from the location 1 sample and 4% from location 2. The Langmuir isotherm model gave a good description of lanthanum adsorption onto BPN, while gadolinium adsorption can be described by both, the Langmuir and Freundlich isotherm models. Considering the availability of banana peels as a waste material and the competitive sorption capacity achieved through milling, this material can be a potential candidate for treatment of lanthanides contaminated mine water.

Acknowledgements One of the authors, Opeyemi A. Oyewo, thanks the National Research Foundation (NRF) of South Africa for offering postgraduate scholarship. Dr Mondiu O. Durowoju and Dr Saliou Diouf are appreciated for their assistance in material characterization, Mr. Cleophas M. Achisa and Olga Oleksiienko for our fruitful discussion. The authors would like to thank all who supported this work.

References

Abdel-Galil EA, Ibrahim AB, Abou-Mesalam MM (2016) Sorption behavior of some lanthanides on polyacrylamide stannic molybdophosphate as organic–inorganic composite. Int J Ind Chem 7:231–240

Achak M, Hafidi A, Ouazzani N, Sayadi S, Mandi L (2009) Low cost biosorbent "banana peel" for the removal of phenolic compounds from olive mill wastewater: kinetic and equilibrium studies. J Hazard Mat 166:117–125

Annadurai G, Juang RS, Lee DJ (2003) Adsorption of heavy metals from water using banana and orange peels. Water Sci Technol 47(185):90

Arup R, Jayanta B (2015) Nanotechnology in industrial wastewater treatment. IWA Publishing, London, p 129

Ashok B, Bhagyashree J, Ameeta RK, Smita Z (2010) Banana peel extract mediated novel route for the synthesis of silver nanoparticles. J Coll Surf 368:58–63

Bakiya LK, Sudha PN (2012) Adsorption of copper (II) ion onto chitosan/sisal/banana fiber hybrid composite. J Environ Sci 3:453

Bankar A, Joshi B, Kumar AR, Zinjarde S (2010) Banana peel extract mediated novel route for the synthesis of silver nanoparticles. Colloids Surf A Physicochem Eng Asp 368:58–63

Bushroa AR, Rahbari RG, Masjuki HH, Muhamad MR (2012) Approximation of crystallite size and microstrain via XRD line broadening analysis in TiSiN thin films. Vacuum 86:1107–1112

Castro RSD, Caetano L, Ferreira G, Padilha PM, Saeki MJ, Zara LF, Martines MAU, Castro GR (2011) Banana peel applied to the solid phase extraction of copper and lead from river water: preconcentration of metal ions with a fruit waste. Ind Eng Chem Res 50:3446–3451

Dongbei W, Ling Z, Li W, Baohui Z, Liyan F (2010) Adsorption of lanthanum by magnetic alginate-chitosan gel beads. J Chem Technol Biotechnol 86:345–352

Dorota K, Zbigniew H (2012) Investigation of sorption and separation of lanthanides on the ion exchangers of various types. Ion exchange technologies, UMCS InTech, Int.ed, Cracow

El-Sofany EA (2008) Removal of lanthanum and gadolinium from nitrate medium using Aliquat-336 impregnated onto Amberlite XAD-4. J Hazard Mat 153:948–954

Firas SA (2013) Thorium removal from waste water using Banana peel and employment of waste residue. Adv Nat Sci 7:336–344

Heguang L, Tiehu L, Tingting H, Xing Z (2015) Effect of multi-walled carbon nanotube additive on the microstructure and properties of pitch-derived carbon foams. J Mater Sci 50:7583–7590

Horcas I, Fernández R, Gómez-Rodríguez JM, Gómez-Herrero J, Baró AM (2007) WSxM: A software for scanning probe microscopy and a tool for nanotechnology. Rev Sci Instrum 78:013705

Hossain MA, Ngo HH, Guo WS, Nguyen TV (2012) Biosorption of Cu(II) from water by Banana peel based biosorbent: experiments and models of adsorption and desorption. J Water Sustain 1:87–104

Kondo K, Kamio E (2002) Seperation of rare earth metals with a polymeric microcapsule membrane. Desalination 144:249–254

Marwani HM, Albishri HM, Jalal TA, Soliman EM (2013) Study of isotherm and kinetic models of lanthanum adsorption on activated carbon loaded with recently synthesized Schiff's base. Arab J Chem 2:1878–5352

Mhadhbi M, Khitouni M, Escoda L, Sunol JJ, Dammak M (2010) Characterization of mechanically alloyed nanocrystalline, Fe(Al). J Nanomater. doi:10.1155/2010/712407

Nacer F, Omar A, Didi MA (2014) Lanthanum (III) Removal onto Lewatit TP 214 Resin in nitrate medium: kinetic and thermodynamic study. IOSR J Appl Chem 7:45–52

Naeem A, Westerhoff P, Mustafa S (2007) Vanadium removal by metal (hydr)oxide adsorbents. Water Res 10:37–146

Nwe Nwe S, Lwin TS, Kay TL (2008) Study on extraction of lanthanum oxide from monazite concentrate. Proc World Acad Sci Eng Technol 2:10–20

Oyewo OA, Onyango MS, Wolkersdorfer C (2016) Application of banana peels nanosorbent in the removal of radioactive minerals from real mine water. J Environ Radioact 164:369–376

Pagano G, Guida M, Siciliano A, Oral R, Koçbaş F, Palumbo A, Castellano I, Migliaccio O, Thomas PJ, Trifuoggi M (2016) Comparative toxicities of selected rare earth elements: sea urchin embryogenesis and fertilization damage with redox and cytogenetic effects. Environ Res 147:453–460. doi:10.1016/j.envres.2016.02.031

Rao TP, Biju VM (2000) Trace determination of lanthanides in metallurgical, environmental and geological samples. Crit Rev Anal Chem 30:179–220

Sert Ş, Kütahyali C, İnan S, Talip Z, Çetinkaya B, Eral M (2008) Biosorption of lanthanum and cerium from aqueous solutions by *Platanus orientalis* leaf powder. Hydrometallurgy 90:13–18

Suryanarayana C (2001) Mechanical alloying and milling. Prog Mater Sci 46:1–184

Tatsuya S, Maiko T, Yasuyuki I, Shin-ichi K (2013) Adsorption behaviors of trivalent actinides and lanthanides on pyridine resin in lithium chloride aqueous solution. Radioanal Nucl Chem 292:286–296

Ungar T (2004) Microstructural parameters from X-ray diffraction peak broadening. Scr Mater 51:777–781

Venkateswarlu K, Sandhyarani M, Nellappan TA, Rameshababu N (2014) Estimation of crystallite size, lattice strain and dislocation density of nanocrystalline carbonate substituted hydroxyapatite by X-ray peak variance analysis. Proced Mat Sci 5:212–221

Wolkersdorfer C (2008) Water management at abandoned flooded underground mines—fundamentals, tracer tests, modelling, water treatment. Springer, Heidelberg